IOP Conference Series: Materials Science and Engineering

PAPER • OPEN ACCESS

Modelling of ductile damage in single point incremental forming process using enhanced CDM model

To cite this article: K Zhang *et al* 2022 *IOP Conf. Ser.: Mater. Sci. Eng.* **1270** 012022

IOP Conf. Series: Materials Science and Engineering 1270 (2022) 012022 doi:10.1088/1757-899X/1270/1/012022

Modelling of ductile damage in single point incremental forming process using enhanced CDM model

K Zhang[1], Z M Yue[2], C J Su[1], R Wang[1] and H Badreddine[3]

[1] College of Mechanical and Electronic Engineering, Shandong University of Science and Technology, Qingdao, 266590, P.R. China
[2] School of Mechanical and Electrical Engineering, Shandong University at Weihai, Weihai 264209, P.R. China
[3] ICD/LASMIS, University of Technology of Troyes, UMR 6281, CNRS, Troyes, France
E-mail: kai.zhang@sdust.edu.cn

Abstract. Investigation of the ductile damage in single point incremental forming (SPIF) is necessary for improving the formability during the manufacturing process. In this paper, an enhanced Continuum Damage Mechanics (CDM) model was applied for ductile damage prediction in SPIF process. In particular, the stress state dependence was considered in the damage evolution to improve fracture prediction capability at various loading paths. The enhanced CDM model was implemented into finite element code ABAQUS/Explicit through user subroutine VUMAT. The accuracy of the finite element model to predict the failure during SPIF process was investigated, good agreements were found between the simulation results and the experimental observations.

1. Introduction

The incremental sheet metal forming process is more flexible than conventional sheet metal forming processes, since it could manufacture components with complex geometries without using specified die set. However, the plastic deformation and damage mechanism are quite different from traditional forming process, e.g. stamping, as the tool path changes rapidly during the forming process[1]. In order to avoid cracks formation and improve the formability of the manufactured parts, the deformation mechanism and ductile fracture behavior during SPIF process should be carefully studied[2].

Finite Element (FE) simulation for SPIF is vital to optimize the forming process, the accuracy of the FE simulation results is highly dependent on the constitutive models. Among the proposed plasticity and damage models, the Continuum Damage Mechanics (CDM) model is widely used coupled damage model to predict ductile damage for metal sheets[3]. Since the plasticity and damage effect are fully coupled in the CDM models, they are more conform in physical mechanism than the uncoupled ones. To date, the CDM model has been widely applied to predict occurrence of failure during various metal forming processes. However, the damage evolution and fracture strain at different loading paths vary with the stress states, the classic CDM model could not accurately reproduce the shear dominated fracture behavior[4]. To extend the CDM model to fracture prediction under various stress states, researchers have modified the damage evolution law in CDM model by adding stress triaxiality and Lode parameter in damage potential[5-7], which has enhanced the predictive capability of the CDM model.

Studies on numerical prediction of damage evolution which considers the stress state effect in SPIF process remains few. In this paper, an enhanced fully coupled elasto-plastic-damage model considering stress triaxiality and Lode angle is used to predict the failure during SPIF process of titanium sheet metal. By comparing the numerical simulation to the experimental results, the enhanced CDM model could predict the damage and fracture in SPIF process with high accuracy.

2. Enhanced CDM damage model

The constitutive equations are developed based on Saanouni model under the total energy equivalent assumption. The specific Helmholtz free energy $\Psi\left(\underline{\varepsilon}^e, \underline{\alpha}, r, T, d\right) = \Psi\left(\underline{\tilde{\varepsilon}}^e, \underline{\tilde{\alpha}}, \tilde{r}, T\right)$ is taken as a state potential given:

$$\rho\Psi = \frac{1}{2}\left(1-h(\eta)d^{\gamma}\right)\kappa_e(\underline{\varepsilon}^{eH}:\underline{\varepsilon}^{eH}) + \left(1-h(\eta)d\right)\mu_e(\underline{\varepsilon}^{eD}:\underline{\varepsilon}^{eD}) + \frac{1}{3}\left(1-h(\eta)d\right)C\underline{\alpha}:\underline{\alpha} + \frac{1}{2}\left(1-h(\eta)d^{\gamma}\right)Qr^2 \quad (1)$$

Assuming the non-associative plasticity theory, the quadratic von Mises yield criterion f and plastic dissipation potential F are defined as follows:

Yield criterion: $$f = \frac{\left\|\underline{\sigma}-\underline{X}\right\|_M}{\sqrt{1-h(\eta)d}} - \frac{R}{\sqrt{1-h(\eta)d^{\gamma}}} - \sigma_y \le 0 \quad (2)$$

Plastic potential: $$F = f + \frac{3a(\underline{X}:\underline{X})}{4C\left(1-h(\eta)d\right)} + \frac{bR^2}{2Q\left(1-h(\eta)d^{\gamma}\right)} + F_d,\ F_d = \frac{S(\bar{\theta})}{(s+1)\left(1-h(\eta)d\right)^{\beta}}\left\langle\frac{Y-Y_0}{S(\bar{\theta})}\right\rangle^{(s+1)} \quad (3)$$

Based on the state potential in Eq. (1) and plastic potential in Eq. (3) defined above, the stress-like variables and all the fluxes variables governing the evolution of the dissipative phenomena are derived and given as follows:

- Stress-like variables for state relation

Cauchy stress: $$\underline{\sigma} = \rho\frac{\partial\Psi}{\partial\underline{\varepsilon}^{eH}} + \rho\frac{\partial\Psi}{\partial\underline{\varepsilon}^{eD}} = \underline{\sigma}^H + \underline{S} = \left(1-h(\eta)d\right)\kappa_e\underline{\varepsilon}^{eH} + 2\left(1-h(\eta)d\right)\mu_e\underline{\varepsilon}^{eD} \quad (4)$$

Kinematic hardening: $$\underline{X} = \rho\frac{\partial\Psi}{\partial\underline{\alpha}} = \frac{2}{3}(1-h(\eta)d)C\underline{\alpha} \quad (5)$$

Isotropic hardening: $$R = \rho\frac{\partial\Psi}{\partial r} = (1-h(\eta)d^{\gamma})Qr \quad (6)$$

Damage force: $$Y = -\rho\frac{\partial\Psi}{\partial d} = \frac{1}{2}h(\eta)\kappa_e(\underline{\varepsilon}^{eH}:\underline{\varepsilon}^{eH}) + \frac{1}{3}h(\eta)C\underline{\alpha}:\underline{\alpha} + h(\eta)\mu_e\left(\underline{\varepsilon}^{eD}:\underline{\varepsilon}^{eD}\right) + \frac{1}{2}h(\eta)\gamma d^{\gamma-1}Qr^2 \quad (7)$$

- Strain-like variables for evolution equation

Plastic strain rate: $$\underline{D}^p = \dot{\lambda}\frac{\partial F}{\partial\underline{\sigma}} = \dot{\lambda}\underline{n} = \frac{\dot{\lambda}}{\sqrt{1-h(\eta)d}}\underline{\tilde{n}},\ \underline{\tilde{n}} = \frac{3\left(\underline{S}-\underline{X}\right)}{2\left\|\underline{\sigma}-\underline{X}\right\|_M} \quad (8)$$

Kinematic hardening strain rate: $$\underline{\dot{\alpha}} = -\dot{\lambda}\frac{\partial F}{\partial\underline{X}} = \dot{\lambda}\left(\frac{\underline{\tilde{n}}}{\sqrt{1-h(\eta)d}} - a\underline{\alpha}\right) \quad (9)$$

Isotropic hardening strain rate: $$\dot{r} = -\dot{\lambda}\frac{\partial F}{\partial R} = \dot{\lambda}\left(\frac{1}{\sqrt{1-h(\eta)d^{\gamma}}} - br\right) \quad (10)$$

Isotropic damage rate: $$\dot{d} = \dot{\lambda}\frac{\partial F}{\partial Y} = \frac{\dot{\lambda}}{(1-h(\eta)d)^{\beta}}\left(\frac{\langle Y-Y_0\rangle}{S(\bar{\theta})}\right)^s \quad (11)$$

In these equations κ_e is the compressibility modulus, μ_e and λ_e are the Lame's constants, E and ν are the Young's modulus and the Poisson's ratio, C, a, Q and b are the kinematic and isotropic hardening moduli, and $S\left(\bar{\theta}\right), s, Y_0, \beta$ and γ are damage parameters.

In the enhanced CDM model, the damage parameter $S\left(\bar{\theta}\right)$ is dependent on the normalized Lode angle $\bar{\theta}$ to obtain different damage evolution under tension and shear loading paths. The stress triaxialtiy η is embedded into the microcracks closure parameter $h(\eta)$ [7]:

$$S(\bar{\theta}) = S_{sh} + \left(S_{ten} - S_{sh}\right)\tanh(\left|\bar{\theta}\right|^{\xi_s}) \tag{12}$$

$$h(\eta) = \frac{1+h_c}{2} + \frac{1-h_c}{2}\tanh(\xi_h \eta) \tag{13}$$

The normalized Lode angle $\bar{\theta}$ ($-1 \le \bar{\theta} \le 1$) and stress triaxiality are defined as follows:

$$\bar{\theta} = 1 - \frac{6\theta}{\pi} = 1 - \frac{2}{\pi}\arccos\left(\frac{3\sqrt{3}J_3}{2J_2^{3/2}}\right),\ \eta = \frac{tr(\underline{\sigma})}{J_2(\underline{\sigma})} \tag{14}$$

where h_c is the value of h at negative stress triaxiality, S_{sh} and S_{ten} represent the value of S in shear and in tension respectively, while ξ_s and ξ_h are parameters to adjust the effect of $\bar{\theta}$ and η. Figure 1 shows the fracture loci of different CDM models, the original CDM model (Model I) could not correctly describe the fracture locus with respect to the stress triaxiality. When the microcracks closure effect is considered (Model II), the asymmetry of damage accumulation under tensile and compressive loading paths could be captured. Only the model with stress state dependence (Model III) could reproduce the non-monotonic fracture locus to accurately predict the damage under tensile, shear and compressive loading paths. In the following section, the enhanced CDM model is applied for fracture prediction during SPIF process for grade 1 titanium sheet.

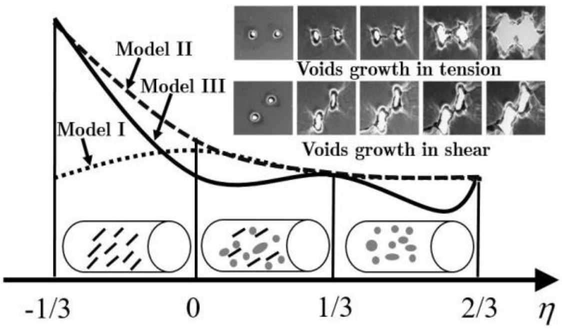

Figure 1. Representation of the fracture loci of different CDM models. (Voids growth photo was taken from reference [9])

3. Parameter identification

In order to simulate the SPIF process, the material parameters for the targeted material should be determined. In this paper, the experimental data for grade 1 pure titanium reported by Gatea et al[10]. was chosen to conduct the simulation. The material parameters are calibrated using tensile and shear tests. The details of the identification methodology could be found in our previous works[7, 8]. The calibrated parameters are given in table 1.

Table 1. Calibrated material parameters for Ti grade 1 sheet.

E (GPa)	υ	σ_y (MPa)	Q (MPa)	b	C (MPa)	a	S_{sh}	S_{ten}
108.0	0.34	232.49	620	1.1	8100	100	46	24

h_c	s	γ	β	Y_0 (MPa)	ξ_s	ξ_h
0.2	1.0	4.0	1.0	0.0	2.0	8.0

Figure 2 shows the comparison of the simulation results and experimental results of tensile and shear tests. The predicted displacements at fracture agree well with the experimental results. Meanwhile, it was found that crack path was in good accordance with the experimental observations for both tensile and shear tests.

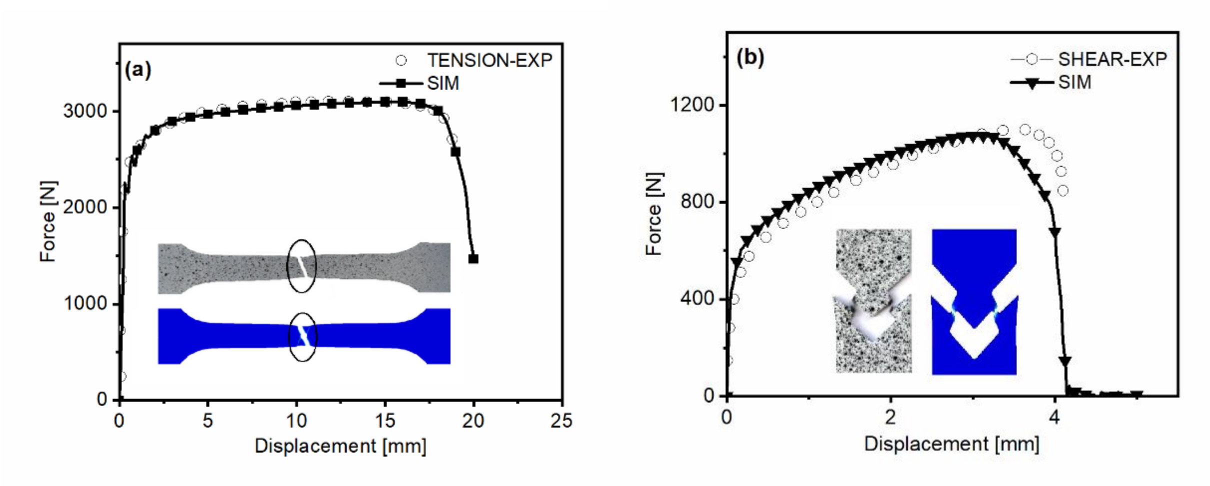

Figure 2. Comparison of force-displacement curves of experimental tests with simulation results based on enhanced CDM model: (a) tensile test; (b) shear test.

4. Numerical simulation of SPIF

To simulate the SPIF process, the finite element model was built according to experimental profile geometry. The mesh of the sheet and tool is shown in figure 3, the dimensions of titanium sheet is 140 ×140×0.7 mm, the diameter of the forming tool is 10 mm. To save the CPU time, only the contact areas are set with fine mesh with element size 0.5 mm. The Coulomb's friction law is selected on contact surface between the tool and the sheet with the friction coefficient of 0.1. Details of the geometric shape of hyperbolic profile can be found in the reference [10]. Next, the SPIF process of hyperbolic shape for grade 1 pure titanium was simulated using enhanced CDM model with the calibrated material parameters in section 3.

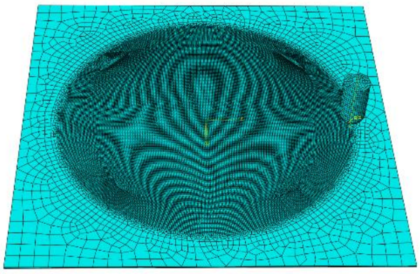

Figure 3. The mesh of the plate and tool.

The distribution of isotropic damage (SDV14) at different forming depths were presented in figure 4, at the beginning, the sheet is without damage, it is noted that the value of isotropic damage is increased when the tool moves along the defined tool path. The isotropic damage localized at the transition area between contact and noncontact areas on the outside of the wall. The maximum value of damage is 0.062 at the forming depth of 14.2 mm. When the forming depth reaches 23.7mm, the damage starts to localize at smaller area on the outside wall of the hyperbolic truncated cone. At forming depth of 31.7 mm, cracks appear at the localized areas, and the value of damage reaches 0.999. It can be seen that the damage is always localized at the outside wall of the hyperbolic truncated cone top corner, where final fracture is observed.

Figure 5 compares the predicted crack path and the fracture depth of the SPIF with the experiments. It is shown that the predicted crack path was in consistent with the actual experiments[10]. In addition, the predicted forming depth (31.7 mm) at fracture was in good agreement with the experimental result (31.1 mm) reported by Gatea et al[10]. From all the comparison of simulation results and experiments, the enhanced CDM damage model could correctly predict the damage evolution and fracture of SPIF process.

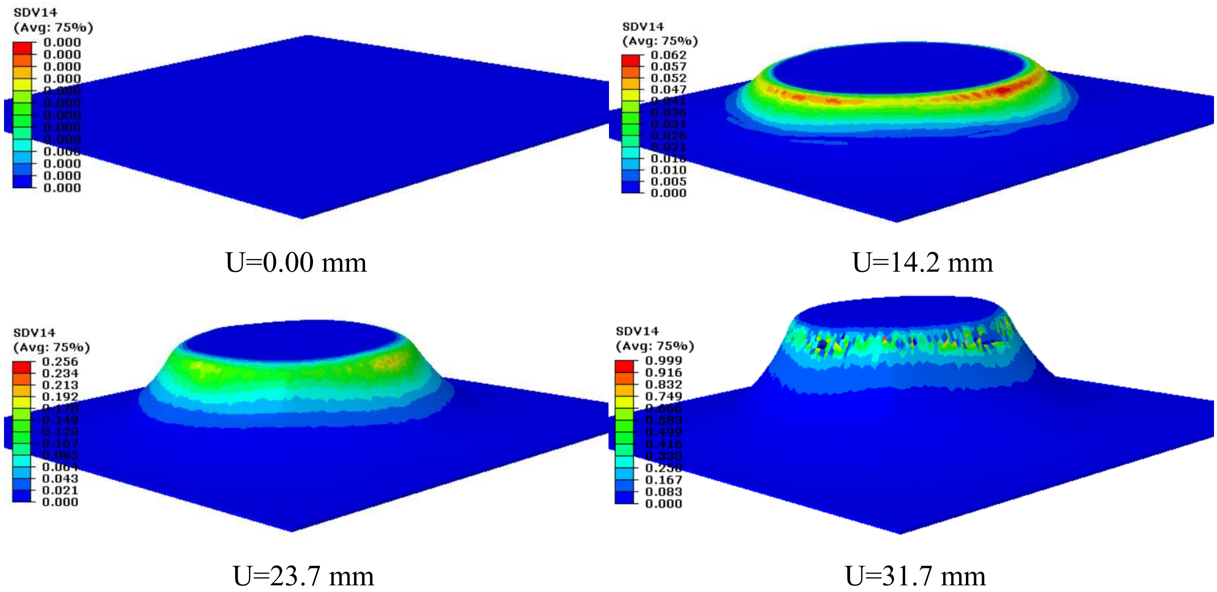

Figure 4. Distribution of isotropic damage (SDV14) during the SPIF forming process of hyperbolic shape.

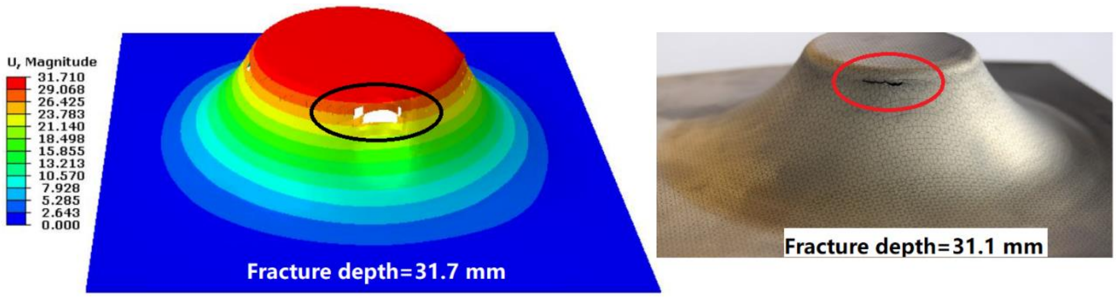

Figure 5. Predicted crack path using the enhanced CDM model in comparison with experiment of the hyperbolic truncated cone SPIF process. (Experimental results is taken from Gatea et al[10])

5. Conclusion

In this paper, an enhanced fully coupled CDM model was applied to simulate the SPIF process of hyperbolic truncated cone for grade 1 pure titanium sheet metal. The model is based on von Mises yield criteria with non-linear mixed isotropic and kinematic hardening. Stress state effect is included in the damage evolution to predict accurately the damage at different loading paths. The material parameters were identified using inverse method. Through comparison of numerical and experimental investigations, it is concluded that the enhanced CDM model could predict the fracture depth and crack path of SPIF process with high accuracy.

References

[1] Su C, Lv S, Wang R, Lv Y, Lou S, Wang Q and Guo S 2021 *Int J Adv Manuf Tech*. **113** 483-501
[2] Zhan X, Wang Z, Li M, Hu Q and Chen J 2020 *J Mater Process Technol*. **282** 116687
[3] Ghorbel O, Mars J, Koubaa S, Wali M and Dammak F 2019 *Int J Mech Sci* **150** 548-60
[4] Bouchard P O, Bourgeon L, Fayolle S and Mocellin K 2010 *Int J Mater Form*. **4** 299-315
[5] Cao T S, Gachet J M, Montmitonnet P and Bouchard P O 2014 *Eng Fract Mech*. **124-125**: 80-96

[6] Malcher L, Mamiya E N 2014 *Int J Plast* **56** 232-261
[7] Zhang K, Badreddine H, Hfaiedh N, Saanouni K and Liu J 2021 *Int J Damage Mech*. **30** 260-282.
[8] Yue Z, Min X, Tuo Z, Soyarslan C, Zhuang X, Badreddine H, Saanouni K and Gao J 2021 *Mat Sci Eng A-Struct* **811** 140978
[9] Weck A and Wilkinson D S 2008 *Acta Mater*. **56** 1774-84
[10] Gatea S, Ou H, Lu B and McCartney G 2017 *Eng. Fract. Mech*. **186** 59-79

Acknowledgments

K.Z. gratefully acknowledges financial support through Project of Shandong Province Higher Educational Young Innovative Talent Introduction and Cultivation Team (Intelligent Transportation Team of Offshore Products)